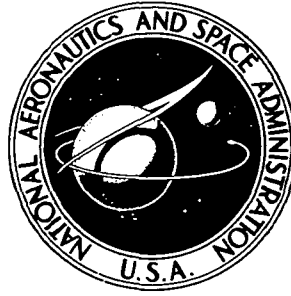


**NASA TECHNICAL
MEMORANDUM**



NASA TM X-3484

NASA TM X-3484

**APPLICATION OF DIFFERENTIAL SIMILARITY
TO FINDING NONDIMENSIONAL GROUPS IMPORTANT
IN TESTS OF COOLED ENGINE COMPONENTS**

James Sucec

Lewis Research Center

Cleveland, Ohio 44135

1. Report No. NASA TM X-3484		2. Government Accession No.		3. Recipient's Catalog No.	
4. Title and Subtitle APPLICATION OF DIFFERENTIAL SIMILARITY TO FINDING NONDIMENSIONAL GROUPS IMPORTANT IN TESTS OF COOLED ENGINE COMPONENTS				5. Report Date March 1977	
				6. Performing Organization Code	
7. Author(s) James Sucec				8. Performing Organization Report No. E-8943	
9. Performing Organization Name and Address Lewis Research Center National Aeronautics and Space Administration Cleveland, Ohio 44135				10. Work Unit No. 505-04	
				11. Contract or Grant No.	
12. Sponsoring Agency Name and Address National Aeronautics and Space Administration Washington, D.C. 20546				13. Type of Report and Period Covered Technical Memorandum	
				14. Sponsoring Agency Code	
15. Supplementary Notes					
16. Abstract <p>The method of differential similarity is applied to the partial differential equations and boundary conditions which govern the temperature, velocity, and pressure fields in the flowing gases and the solid stationary components in air-cooled engines. This procedure yields the nondimensional groups which must have the same value in both the test rig and the engine to produce similarity between the test results and the engine performance. These results guide the experimentalist in the design and selection of test equipment that properly scales quantities to actual engine conditions. They also provide a firm fundamental foundation for substantiation of previous similarity analyses which employed heuristic, physical reasoning arguments to arrive at the nondimensional groups.</p>					
17. Key Words (Suggested by Author(s)) Similarity conditions Gas turbines Turbine temperatures Aircraft engines				18. Distribution Statement Unclassified - unlimited STAR Category 07	
19. Security Classif. (of this report) Unclassified		20. Security Classif. (of this page) Unclassified		22. Price* \$4.00	
				21. No. of Pages 35	

* For sale by the National Technical Information Service, Springfield, Virginia 22161

APPLICATION OF DIFFERENTIAL SIMILARITY TO FINDING NONDIMENSIONAL GROUPS IMPORTANT IN TESTS OF COOLED ENGINE COMPONENTS

by James Sucec*

Lewis Research Center

SUMMARY

The nondimensional groups required for similarity of flow and heat transfer in cooled engine components between a test rig and an engine are found by the application of the method of differential similarity to the governing partial differential equations and their boundary conditions for the hot gas, cooled metal, and coolant gas. The most important of these groups required for similarity are geometric variables; Mach, Reynolds, and Prandtl numbers; the ratio of coolant to hot gas mass flow rate, the ratio of coolant to hot gas temperature, and the turbulence intensity of the free stream. Suitable rearrangement of these groups makes it possible to arrive at the nondimensional groups normally used in tests of cooled engine components. The work in this report provides a sound theoretical basis for use of these groups, which were selected in the past on the basis of heuristic, physical insight arguments and also because they are often the groups the experimenter has most control over.

Differential similarity also uncovers some groups to which scant, if any, attention has been paid in the past. Apparently, these groups exercise a second order effect, at best. In addition, differential similarity is applied formally to two turbulent shear stress models, which causes the turbulence intensity of the free stream to surface as a nondimensional group.

INTRODUCTION

The work employs the technique of differential similarity to find the nondimensional groups which must have the same value for both a test rig and a cooled engine part in order that engine heat-transfer performance be properly modelled by a test rig.

* Professor of Mechanical Engineering, University of Maine, Orono, Maine; Summer Faculty Fellow at the Lewis Research Center in 1973.

Often cooled engine components are tested at relatively low temperatures and pressures so that instrumentation and test equipment can be less complex and constructed less expensively than they would be for a test at the high-temperature, high-pressure engine conditions. Sometimes it is convenient to work with the full-scale hardware, for instance, when one is interested in the temperatures in a first stage vane. At other times a larger than prototype size scale model may be dictated by a desire to investigate more detailed, basic phenomena such as the influence of a pressure gradient on the film effectiveness very near a film slot on a surface. In both cases one must be able to design the test rig properly and then scale the experimental information collected from the test so as to predict prototype behavior. This requires that the test rig (model) be similar to the engine component (prototype).

One necessary condition for this similarity is geometric similarity, that is, the use of a scale model. The other conditions for similarity can be found in a number of ways including the use of the Buckingham pi theorem, examination of available exact analytical solutions to closely related problems, use of physical insight and reasoning, and examination of the governing partial differential equations and the boundary conditions. This last technique can be employed even though the equations and boundary conditions may not be presently amenable to an exact analytical solution. In reference 1 a combination of physical reasoning and some nondimensional groups presented in reference 2 leads to some of the conditions necessary for similarity. The groups used and the scaling procedure recommended are checked by comparing measured airfoil temperatures at high gas temperature and pressure with scaled up values based on tests at low gas temperature and pressure. The agreement seems reasonable in the range of conditions explored. Chapter 11 of reference 3 presents similarity conditions based on heuristic arguments, physical insight, and the author's experience and knowledge of what is important when investigating forced convection heat-transfer phenomena. Two tables of similarity states valid for a high-performance jet engine at takeoff conditions and at cruise conditions are presented. Reference 4 is a much more detailed and expanded version of the similarity material presented in reference 3. The basis for selection of the appropriate nondimensional groups is still the same as in reference 3, and the steps one would follow in using them are thoroughly explained. In addition, the authors emphasize some of the pitfalls that await those who violate the major constraints imposed by similarity requirements. The authors point out the serious errors that can occur if one fallaciously reasons that cooling performance can be demonstrated by a test at near prototype temperatures but at low pressures very near the standard atmosphere. The procedures and the caveats advanced in reference 4 constitute an invaluable addition to the literature for those involved in testing the cooled components of the engine. However, there is still a gap in the general area of a rigorous foundation for the nondimensional groups which are sufficient for similarity.

This report uses a rigorous mathematical method, differential similarity, on an idealized but still fairly general physical model to find the nondimensional groups required for similarity. Once these groups are found, they are examined to see if they imply the groups found by the less rigorous approach of reference 4; since they do, they can serve as the underlying framework of the structure presented there. Additionally, differential similarity is formally and explicitly applied to some turbulent shear stress models to see if any additional groups appear over and above those which exist in a purely laminar flow.

ANALYSIS OF STEADY, LAMINAR FLOW

To find the nondimensional groups which ensure similarity by the use of differential similarity, one writes down all the partial differential equations, the algebraic equations, and the side conditions that govern the solution of the problem at hand; makes all equations and side conditions nondimensional; and then by direct inspection writes down the implicit functional dependence of all the dependent nondimensional groups upon the independent groups and the other nondimensional parameters. For more detail, one may wish to consult references 5 and 6.

Although the results of the following analysis are valid for most air-cooled stationary components of an engine, the following idealized model is considered for concreteness. A hot gas flows in a steady, laminar fashion through a cascade of stationary metal vanes inside of which a coolant gas flows in a steady and laminar mode. Body forces are neglected, and both the gas and coolant are assumed to obey the perfect gas equation of state, have internal energy per unit mass and enthalpy per unit mass which depend only on temperature, have a dynamic viscosity which is only temperature dependent, and behave as linearly viscous fluids in regard to their viscous stresses. For simplicity, the thermal conductivity, dynamic viscosity, and specific heat of both the gas and the coolant have their temperature dependence given by power law forms. The metal is considered rigid and isotropic, and a power law form is used for the temperature dependence of its thermal conductivity. Gas radiation effects and mass diffusional effects are not dealt with. These constraints define the idealized model which is now rigorously analyzed for the nondimensional groups which ensure similarity between engine conditions and test conditions.

Later the generalization to steady turbulent flow is made, and this requires additional assumptions to be invoked because of the need for a choice of turbulence model.

A schematic of one of the vanes under consideration and some of the associated nomenclature are presented in figure 1. (All symbols are defined in appendix A.)

The governing equations for the flowing hot gas are as follows:

Conservation of mass:

$$\frac{\partial(\rho u)}{\partial x} + \frac{\partial(\rho v)}{\partial y} + \frac{\partial(\rho w)}{\partial z} = 0 \quad (1)$$

x-direction Navier-Stokes (see ref. 7):

$$\begin{aligned} \rho \left(u \frac{\partial u}{\partial x} + v \frac{\partial u}{\partial y} + w \frac{\partial u}{\partial z} \right) = & - \frac{\partial P}{\partial x} + \frac{\partial}{\partial x} \left\{ \mu \left[2 \frac{\partial u}{\partial x} - \frac{2}{3} \left(\frac{\partial u}{\partial x} + \frac{\partial v}{\partial y} + \frac{\partial w}{\partial z} \right) \right] \right\} \\ & + \frac{\partial}{\partial y} \left[\mu \left(\frac{\partial u}{\partial y} + \frac{\partial v}{\partial x} \right) \right] + \frac{\partial}{\partial z} \left[\mu \left(\frac{\partial w}{\partial x} + \frac{\partial u}{\partial z} \right) \right] \end{aligned} \quad (2)$$

(The Navier-Stokes equations for the y- and z-directions are similar in form to eq. (2) and are not shown since they do not yield any nondimensional groups that are different from those which can be extracted from eq. (2).)

Thermal energy:

$$\begin{aligned} \rho c_p \left(u \frac{\partial T}{\partial x} + v \frac{\partial T}{\partial y} + w \frac{\partial T}{\partial z} \right) = & \frac{\partial}{\partial x} \left(k \frac{\partial T}{\partial x} \right) + \frac{\partial}{\partial y} \left(k \frac{\partial T}{\partial y} \right) + \frac{\partial}{\partial z} \left(k \frac{\partial T}{\partial z} \right) \\ & + u \frac{\partial P}{\partial x} + v \frac{\partial P}{\partial y} + w \frac{\partial P}{\partial z} + \mu \Phi \end{aligned} \quad (3)$$

$$\begin{aligned} \Phi = & 2 \left[\left(\frac{\partial u}{\partial x} \right)^2 + \left(\frac{\partial v}{\partial y} \right)^2 + \left(\frac{\partial w}{\partial z} \right)^2 \right] + \left(\frac{\partial u}{\partial y} + \frac{\partial v}{\partial x} \right)^2 + \left(\frac{\partial v}{\partial z} + \frac{\partial w}{\partial y} \right)^2 \\ & + \left(\frac{\partial w}{\partial x} + \frac{\partial u}{\partial z} \right)^2 - \frac{2}{3} \left(\frac{\partial u}{\partial x} + \frac{\partial v}{\partial y} + \frac{\partial w}{\partial z} \right)^2 \end{aligned}$$

State:

$$\rho = \frac{P}{RT} \quad (4)$$

$$i - i_{\text{ref}} = \int_{T_{\text{ref}}}^T c_p(\xi) d\xi \quad (5)$$

It is assumed that the temperature dependent fluid properties, dynamic viscosity μ , thermal conductivity k , and specific heat at constant pressure c_p can be adequately represented in the temperature range of interest by the following power law forms:

$$\mu(T) = \mu_0 \left(\frac{T}{T_0} \right)^d \quad (6)$$

$$k(T) = k_0 \left(\frac{T}{T_0} \right)^g \quad (7)$$

$$c_p(T) = c_{p,\infty} \left(\frac{T}{T_\infty} \right)^l \quad (8)$$

For the metal, which is assumed isotropic and rigid, one has the following equations:

$$\frac{\partial}{\partial x} \left(k_m \frac{\partial T_m}{\partial x} \right) + \frac{\partial}{\partial y} \left(k_m \frac{\partial T_m}{\partial y} \right) + \frac{\partial}{\partial z} \left(k_m \frac{\partial T_m}{\partial z} \right) = 0 \quad (9)$$

$$k_m = k_{m0} \left(\frac{T_m}{T_0} \right)^b \quad (10)$$

For the coolant one has equations that are the same as equations (1) to (5) with all quantities except the independent variables x , y , and z having a subscript c to identify them as being local values within the coolant. Hence, the equations for the coolant are not shown explicitly. Also, for the coolant we have

$$\mu_c = \mu_{c,0} \left(\frac{T_c}{T_0} \right)^{d_c} \quad (11)$$

$$k_c = k_{c,0} \left(\frac{T_c}{T_0} \right)^{g_c} \quad (12)$$

$$c_{p,c} = c_{p,\infty,c} \left(\frac{T_c}{T_\infty} \right)^{l_c} \quad (13)$$

At this point it might be noted that the coordinate system shown in figure 1 is rectangular Cartesian, so that the governing partial differential equations are relatively simple and have no curvature terms. In the event that the circumstances allow thin-boundary-layer flow, the coordinate system can be viewed as a curvilinear one which follows the vane surface.

The boundary conditions must be written down. For the hot gas as $x \rightarrow -\infty$

$$\left. \begin{aligned} u &= u_\infty & P &= P_\infty \\ v &= 0 & T &= T_\infty \\ w &= 0 \end{aligned} \right\} \quad (14)$$

On all solid surfaces

$$u = v = w = 0 \quad (15)$$

and downstream in the gas as $x \rightarrow \infty$

$$\left. \begin{aligned} \frac{\partial u}{\partial x} = \frac{\partial v}{\partial y} = \frac{\partial w}{\partial z} &= 0 \\ \frac{\partial T}{\partial x} &= 0 \end{aligned} \right\} \quad (16)$$

(Note that a precise specification of the downstream boundary, $x \rightarrow \infty$, is not important unless the velocity and temperature fields are strongly elliptic in the x -direction. If the flow is of the thin-boundary-layer type, nothing need be specified as $x \rightarrow \infty$, since the equations are then parabolic in x . Hence, in eq. (16) relatively weak conditions are used on the downstream boundary.)

For the coolant the boundary conditions are

$$\left. \begin{array}{ll} z = 0 & P_c = P_{ci} \\ u_c = v_c = 0 & T_c = T_{ci} \\ w_c = w_{ci} & \end{array} \right\} \quad (17)$$

On all solid surfaces

$$u_c = v_c = w_c = 0 \quad (18)$$

The remarks previously made in connection with the downstream boundary for the hot gas are taken as applicable to the coolant as well.

At the interface between the gas and the solid metal the conjugation conditions are

$$T = T_m \quad (19)$$

$$-k_m \frac{\partial T_m}{\partial n} = -k \frac{\partial T}{\partial n} + \epsilon_m \sigma \left(T_m^4 - \sum_{j=1}^p B_{m,j} T_j^4 \right) \quad (20)$$

The second term on the right side of equation (20) represents the net radiant loss per unit area by the metal due to gray body radiant exchange with solid surfaces. In this term $B_{m,j}$ is Gebhart's absorption factor, the fraction of the radiant energy emitted by the surface m which is ultimately absorbed by the j^{th} surface.

Two conjugation conditions of the form of equations (19) and (20) also hold for the interface between the coolant gas and the metal.

Equations (1) to (20) are made nondimensional by dividing all velocities, whether in hot gas or coolant, by u_∞ (hot gas velocity upstream of cooled component); dividing all temperatures, hot gas, coolant gas, and metal, by T_0 (inlet stagnation temperature of hot gas); and dividing all space coordinates by the characteristic length L , which is chosen as the airfoil chord in this report. Also, pressure and density are made dimensionless through division by P_∞ and ρ_∞ , respectively, the static conditions at the hot gas inlet. Differential similarity methods next require formal transformation of the dimensional dependent and independent variables to the nondimensional ones in all the equations. Once this is complete, the equations are made nondimensional. A representative illustration of this procedure is presented in appendix B.

When equations (6) to (8) are combined with equations (2) and (3), equations (11) to (13) are combined with the counterparts of equations (2) and (3) for the coolant, and

equation (10) is inserted into (9), the method of differential similarity finally yields the following nondimensional equations:

For the hot gas:

Conservation of mass:

$$\frac{\partial(\hat{\rho}U)}{\partial X} + \frac{\partial(\hat{\rho}V)}{\partial Y} + \frac{\partial(\hat{\rho}W)}{\partial Z} = 0 \quad (21)$$

x-direction Navier-Stokes:

$$\hat{\rho} \left(U \frac{\partial U}{\partial X} + V \frac{\partial U}{\partial Y} + W \frac{\partial U}{\partial Z} \right) = -Eu \frac{\partial \hat{P}}{\partial X} + \frac{1}{Re} \frac{\partial}{\partial X} \left[\theta^d \left(2 \frac{\partial U}{\partial X} + \text{other velocity gradient terms} \right) \right] \quad (22)$$

Thermal energy:

$$\begin{aligned} \hat{\rho} \theta^l \left(\frac{T_0}{T_\infty} \right)^l \left(U \frac{\partial \theta}{\partial X} + \dots \right) &= \frac{1}{RePr} \left[\frac{\partial}{\partial X} \left(\theta^g \frac{\partial \theta}{\partial X} \right) + \dots \right] \\ &+ EuEc \left(U \frac{\partial \hat{P}}{\partial X} + \dots \right) + \frac{Ec}{Re} \theta^d \left[2 \left(\frac{\partial U}{\partial X} \right)^2 + \dots \right] \end{aligned} \quad (23)$$

For the sake of compactness of form, terms with the same general form and characteristics, such as the three terms in parentheses on the left side of equation (22), are often represented by + ... This, of course, is no loss once all the nondimensional dependent and independent variables have appeared, since these additional terms do not contribute any new nondimensional groups.

State:

$$\hat{\rho} = \frac{\hat{P}}{\theta} EuEc \frac{c_{p,\infty}}{R} \quad (24)$$

For the metal:

$$\frac{\partial}{\partial X} \left(\theta_m^b \frac{\partial \theta_m}{\partial X} \right) + \dots = 0 \quad (25)$$

For the coolant:

Conservation of mass:

$$\frac{\partial}{\partial X} (\hat{\rho}_c U_c) + \dots = 0 \quad (26)$$

x-direction Navier-Stokes:

$$\hat{\rho}_c \left(U_c \frac{\partial U_c}{\partial X} + \dots \right) = -Eu \frac{\partial \hat{P}_c}{\partial X} + \frac{\mu_{c,0}}{\mu_0} \frac{1}{Re} \frac{1}{\partial X} \left[\theta_c^d \left(2 \frac{\partial U_c}{\partial X} + \dots \right) \right] \quad (27)$$

Thermal energy:

$$\begin{aligned} \hat{\rho}_c \left(\theta_c \frac{T_0}{T_\infty} \right)^{l_c} \left(U_c \frac{\partial \theta_c}{\partial X} + \dots \right) &= \frac{k_{c,0}}{Re} \frac{c_{p,\infty}}{Pr} \frac{\partial}{\partial X} \left[\left(\theta_c^g \frac{\partial \theta_c}{\partial X} + \dots \right) \right] \\ &+ \frac{c_{p,\infty}}{c_{p,\infty,c}} Eu Ec \left(U_c \frac{\partial \hat{P}_c}{\partial X} + \dots \right) + \frac{\mu_{c,0}}{\mu_0} \frac{c_{p,\infty}}{c_{p,\infty,c}} \frac{Ec}{Re} \theta_c^d \left[2 \left(\frac{\partial U_c}{\partial X} \right)^2 + \dots \right] \end{aligned} \quad (28)$$

State:

$$\hat{\rho}_c = \frac{\hat{P}_c}{\theta_c} \frac{R}{R_c} \frac{T_\infty}{T_0} \quad (29)$$

The nondimensional boundary conditions for the hot gas are

As $X \rightarrow -\infty$

$$U = 1 \quad V = 0 \quad W = 0$$

$$\hat{P} = 1 \quad \theta = \frac{T_\infty}{T_0}$$

As $X \rightarrow \infty$

$$\frac{\partial U}{\partial X} = \frac{\partial V}{\partial Y} = \frac{\partial W}{\partial Z} = \frac{\partial \theta}{\partial X} = 0$$

On solid surfaces

$$U = V = W = 0$$

(30)

In the coolant the boundary conditions are

At $Z = 0$

$$\left. \begin{aligned} W_c &= \frac{w_{ci}}{U_\infty} & \theta_c &= \frac{T_{ci}}{T_0} \\ V_c &= 0 & \hat{P} &= \frac{P_{ci}}{P_\infty} \\ U_c &= 0 \end{aligned} \right\} \quad (31)$$

On solid surfaces

$$U_c = V_c = W_c = 0$$

Conjugation conditions on solid surfaces are

$\theta = \theta_m$ and

$$\left. \begin{aligned} -\frac{k_{m0}}{k_0} \left(\theta_m^b \frac{\partial \theta_m}{\partial N_0} \right)_{N_0=0} &= - \left(\theta_m^g \frac{\partial \theta}{\partial N_0} \right)_{N_0=0} + \frac{\epsilon_m \sigma T_0^4}{k_0} \theta_m^4 - \sum_{j=1}^p \frac{\epsilon_m \sigma T_0^4}{k_0} B_{m,j} \theta_j^4 \\ \text{Also, } \theta_c &= \theta_m \text{ and} \end{aligned} \right\} \quad (32)$$

$$\left. \begin{aligned} -\frac{k_{m0}}{k_{c,0}} \left(\theta_m^b \frac{\partial \theta_m}{\partial m_o} \right)_{m_o=0} &= - \left(\theta_c^g \frac{\partial \theta_c}{\partial m_o} \right)_{m_o=0} + \frac{\epsilon_m \sigma T_0^4}{k_{c,0}} \theta_m^4 - \sum_{j=1}^{p_c} \frac{\epsilon_m \sigma T_0^4}{k_{c,0}} B_{m,j} \theta_j^4 \end{aligned} \right\}$$

Inspection of equations (21) to (32) reveals that the nondimensional dependent variables are a function of the nondimensional independent variables and all nondimensional parameters. Hence,

$$\begin{aligned}
(U, V, W, \hat{P}, \theta, \hat{\rho}, \theta_m, U_c, V_c, W_c, \hat{P}_c, \theta_c, \hat{\rho}_c) = G_i \left[X, Y, Z, Eu, Re, d, l, \frac{T_0}{T_\infty}, Pr, g, \frac{k_{m0}}{k_0}, \right. \\
Ec, \frac{c_{p,\infty}}{R}, b, \frac{\mu_{c,0}}{\mu_0}, d_c, l_c, \frac{k_{c,0}}{k_0}, \frac{c_{p,\infty}}{c_{p,\infty,c}}, g_c, \frac{R}{R_c}, \frac{w_{ci}}{u_\infty}, \frac{T_{ci}}{T_0}, \frac{P_{ci}}{P_\infty}, \frac{\epsilon_m \sigma T_0^4}{k_0}, \\
\left. \frac{\epsilon_m \sigma T_0^4}{k_0} B_{m,j}, \frac{k_{m0}}{k_{c,0}}, \frac{\epsilon_m \sigma T_0^4}{k_{c,0}}, \left(\frac{\epsilon_m \sigma T_0^4}{k_{c,0}} B_{m,j} \right)_c \right] \quad (33)
\end{aligned}$$

where

$$\begin{aligned}
Eu &= \frac{P_\infty}{\rho_\infty u_\infty^2} & Pr &= \frac{\mu_0 c_{p,\infty}}{k_0} \\
Re &= \frac{\rho_\infty u_\infty L}{\mu_0} & Ec &= \frac{u_\infty^2}{c_{p,\infty} T_0}
\end{aligned}$$

The function G_i in equation (33) is different for each of the dependent nondimensional variables on the left side of the equation.

Basically equation (33) means that the nondimensional fields of velocity, temperature, pressure, and density in the hot gas and in the coolant, as well as the nondimensional metal temperature field, are the same in both model and prototype, test rig and engine, if the corresponding nondimensional groups in the test rig and the engine which appear in the argument of the G_i function are the same in the test rig and the engine. In the framework of the problem addressed in this report, this requirement and geometric similarity constitute sufficient conditions for similarity between the test rig and the engine.

EXTENSION TO STEADY ON THE AVERAGE TURBULENT FLOW

As is well known, for a steady turbulent flow, equation (2), for instance, contains additional momentum flux terms due to the fluctuation components of velocity. It is usual to treat these terms as additional apparent stresses, called turbulent, or Reynolds, stresses. To see whether differential similarity will predict any additional nondimensional groups due to turbulence, consider, for the sake of simplicity, the case of

incompressible, thin-boundary-layer flow. Calling the apparent turbulent shearing stress in the x -direction $\tau_{t,x}$, one can show that equation (2) reduces to

$$\rho \left(u \frac{\partial u}{\partial x} + \dots \right) = - \frac{\partial P}{\partial x} + \frac{\partial \tau_{t,x}}{\partial y} + \dots + \frac{\partial}{\partial y} \left(\mu \frac{\partial u}{\partial y} + \dots \right) + \dots \quad (34)$$

As shown in appendix B, for this equation without the turbulent stresses, the non-dimensional form becomes

$$U \frac{\partial U}{\partial X} + \dots = -Eu \frac{\partial \hat{P}}{\partial X} + \frac{1}{Re} \frac{\partial}{\partial Y} \left(\theta^d \frac{\partial U}{\partial Y} + \dots \right) + \dots + \frac{L}{\rho_\infty u_\infty^2} \frac{\partial \tau_{t,x}}{\partial y} + \dots \quad (35)$$

Now if one chooses to use mixing length theory together with an algebraic prescription of the mixing lengths for a boundary layer near a single wall, one obtains the following equations, according to reference 8, page 29:

$$\left. \begin{aligned} \tau_{t,x} &= \rho_\infty (0.41)^2 y^2 \left(\frac{\partial u}{\partial y} \right)^2 & 0 \leq y \leq \frac{0.09}{0.41} \delta \\ \tau_{t,x} &= \rho_\infty (0.09)^2 \delta^2 \left(\frac{\partial u}{\partial y} \right)^2 & \frac{0.09\delta}{0.41} \leq y \leq \delta \end{aligned} \right\} \quad (36)$$

Since $U = u/u_\infty$ and $Y = y/L$ and Δ can be defined as δ/L , equations (36) become

$$\left. \begin{aligned} \tau_{t,x} &= \rho_\infty u_\infty^2 (0.41)^2 Y^2 \left(\frac{\partial U}{\partial Y} \right)^2 \\ \tau_{t,x} &= \rho_\infty u_\infty^2 (0.09)^2 \Delta^2 \left(\frac{\partial U}{\partial Y} \right)^2 \end{aligned} \right\} \quad (37)$$

Differentiating equations (37) with respect to y and then changing to the nondimensional coordinate Y give

$$\left. \begin{aligned} \frac{\partial \tau_{t,x}}{\partial y} &= \frac{\rho_{\infty} u_{\infty}^2}{L} (0.41)^2 \frac{\partial}{\partial Y} \left[Y^2 \left(\frac{\partial U}{\partial Y} \right)^2 \right] \\ \frac{\partial \tau_{t,x}}{\partial y} &= \frac{\rho_{\infty} u_{\infty}^2}{L} (0.09)^2 \Delta^2 \frac{\partial}{\partial Y} \left[\left(\frac{\partial U}{\partial Y} \right)^2 \right] \end{aligned} \right\} \quad (38)$$

When equation (38) is inserted into (35), the $\rho_{\infty} u_{\infty}^2/L$ term cancels, and the nondimensional equation, including the turbulent stresses, has one of the following two forms, depending on the position within the boundary layer:

$$U \frac{\partial U}{\partial X} + \dots = -Eu \frac{\partial \hat{P}}{\partial X} + \frac{1}{Re} \frac{\partial}{\partial Y} \left(\theta^d \frac{\partial U}{\partial Y} + \dots \right) + \dots + \left\{ \begin{aligned} &(0.41)^2 \frac{\partial}{\partial Y} \left[Y^2 \left(\frac{\partial U}{\partial Y} \right)^2 \right] + \dots \\ &(0.09)^2 \Delta^2 \frac{\partial}{\partial Y} \left(\frac{\partial U}{\partial Y} \right)^2 + \dots \end{aligned} \right\} \quad (39)$$

Upon examination of equation (39), one sees that no new groups are introduced by taking explicit account of the turbulent stresses, at least not for the simple turbulence model involving prescription of the mixing length through algebraic equations. (Since Δ is defined as the nondimensional thickness of the boundary layer, it depends on some of the same groups as U and hence introduces no new groups.)

With regard to models for the turbulent shearing stress, the next level of sophistication is the so-called one equation model of turbulence, where a length scale of turbulence and a characteristic scale of the turbulent velocities are used. The length scale is taken to be the usual algebraic mixing length prescription, while the velocity scale used is proportional to the square root of the turbulent kinetic energy. When K is defined as the average turbulent kinetic energy divided by u_{∞}^2 , the nondimensional form of the partial differential equation describing the distribution of K can easily be shown to be

$$U \frac{\partial K}{\partial X} + \dots = \frac{\partial}{\partial Y} \left(\frac{L_{\text{mix}} \sqrt{K}}{\sigma_k} \frac{\partial K}{\partial Y} \right) + L_{\text{mix}} \sqrt{K} \left(\frac{\partial U}{\partial Y} \right)^2 - \frac{C_D K^{3/2}}{L_{\text{mix}}} \quad (40)$$

(See ref. 8 for the dimensional version of the turbulent kinetic energy equation.)

The boundary conditions in nondimensional form for this equation are

On all solid surfaces

As $X \rightarrow \infty$

$$K = 0$$

$$\frac{\partial K}{\partial X} = 0$$

As $X \rightarrow -\infty$

$$K = K_{\infty}$$

(41)

In equation (40), L_{mix} is the nondimensional mixing length, and reference to equation (39) and the immediately preceeding work indicates that the presence of L_{mix} does not give rise to any new groups. However, equation (40) gives one new dependent group, K , to be added to the groups on the left side of equation (33). The C_D in equation (40) is a pure number, while σ_k is a sort of turbulent Prandtl number for turbulent kinetic energy. It is the ratio of the eddy diffusivity of momentum to the eddy diffusivity of turbulent kinetic energy. This σ_k and the ordinary turbulent Prandtl number σ_t are two additional groups that should be added to the right side of equation (33); σ_t appears in the nondimensional thermal energy equation for turbulent flow when one relates the turbulent transport coefficients of heat and momentum. Also, the nondimensional boundary conditions lead to a new group to be added to the right side, namely, K_{∞} . But K_{∞} is a multiple of the more common turbulence parameter, the turbulence intensity TI_{∞} , so this is used in its place.

In appendix C it is shown that T_0/T_{∞} , Eu , and Ec are functions of inlet gas Mach number M_{∞} , of l , and of $c_{p,\infty}/R$, which itself depends on the specific heat ratio of the hot inlet gas. Utilizing these results and the ones just derived for turbulent flow, one obtains

$$(U, V, W, \hat{P}, \theta, \hat{\rho}, \theta_m, U_c, V_c, W_c, \hat{P}_c, \theta_c, \hat{\rho}_c, K) =$$

$$F_i \left[X, Y, Z, Re, Pr, M_\infty, d, l, g, \frac{c_{p,\infty}}{R}, b, \frac{k_{m0}}{k_0}, \frac{\mu_{c,0}}{\mu_0}, d_c, l_c, \frac{k_{c,0}}{k_0}, \frac{c_{p,\infty}}{c_{p,\infty,c}}, \right. \\ \left. g_c, \frac{R}{R_c}, \frac{w_{ci}}{u_\infty}, \frac{T_{ci}}{T_0}, \frac{P_{ci}}{P_\infty}, \frac{\epsilon_m^\sigma T_0^4}{k_0}, \frac{\epsilon_m^\sigma T_0^4}{k_0} B_{m,j}, \frac{k_{m0}}{k_{c,0}}, \frac{\epsilon_m^\sigma T_0^4}{k_{c,0}}, \right. \\ \left. \left(\frac{\epsilon_m^\sigma T_0^4}{k_{c,0}} B_{m,j} \right)_c, \sigma_k, \sigma_t, Tl_\infty \right] \quad (42)$$

The function F_i is different for each of the nondimensional dependent variables.

RESULTS AND DISCUSSION

One of the major results of this analysis is equation (42); for a test rig and an engine that are geometrically similar this equation gives the sufficient conditions for equality of the nondimensional temperature, pressure, density, and velocity fields in the hot gas, the metal, and the coolant. These sufficient conditions for similarity between the test rig and the engine are the equality, in the test rig and in the engine, of every nondimensional group in the argument of the functions on the right side of equation (42). As is generally true, one can have strict similarity, that is, meet all the conditions for similarity, only if the test rig is the actual engine operating under actual engine conditions. However, as mentioned previously, many of these requirements exert only a slight influence on the dependent variables and sometimes may safely be dispensed with. Brief arguments are now presented for the dropping of many of these constraints. In this discussion the superscript t refers to the test rig (model), and the superscript e refers to the engine (prototype).

Perhaps the most convincing argument that many of the groups on the right side of equation (42) exert only a weak influence on similarity between the test rig and the engine, and on proper scaling, is that tests have been run without equality between the test rig and the engine for many of the groups and that direct experiment has shown that the lower pressure and temperature data do scale up and agree well with the measured values at engine conditions. This is shown in reference 1.

One of the requirements for strict similarity from equation (42) is that

$$d^t = d^e \quad (43)$$

That is, the exponent on the power law fit to the temperature dependent dynamic viscosity of the hot gas must be the same in the test rig as in the engine. A plot of the dynamic viscosity of air from the values given in reference 5 yields the conclusion that a single choice of d in equation (6) adequately represents μ over a wide temperature range. Hence, use of air in both the test rig and the engine tends to guarantee at least approximate equality of the two members in equation (43). If air is also the coolant, it seems reasonable to suppose that the nondimensional groups d , l , g , $c_{p,\infty}/R$, $\mu_{c,0}/\mu_0$, d_c , l_c , $k_{c,0}/k_0$, $c_{p,\infty}/c_{p,c}$, g_c , and R/R_c would have the same value in both the test rig and the engine.

Another ameliorative influence is the fact that satisfying the most important conditions for similarity ensures the same temperature ratio across the boundary layer at corresponding points in the test rig and the engine. This condition gives the correct effect of temperature dependent properties on both the surface coefficient of heat transfer and the wall shearing stress for a large number of different gases, as is pointed out in reference 7. The available experimental evidence and the present thinking (ref. 8) indicate that σ_k and σ_t are practically equal and do not vary much from fluid to fluid except for the extreme Prandtl number fluids such as liquid metals and hydrocarbon oils, neither of which would be used as the test fluid for the engine hot gas or the engine coolant. Hence, the equalities that follow are automatically satisfied:

$$\left. \begin{aligned} \sigma_k^t &= \sigma_k^e \\ \sigma_t^t &= \sigma_t^e \end{aligned} \right\} \quad (44)$$

It is usual to select test fluids and materials that are close enough to engine conditions to allow the following equalities:

$$\left(\frac{k_{m0}}{k_0} \right)^t = \left(\frac{k_{m0}}{k_0} \right)^e \quad (45a)$$

$$b^t = b^e \quad (45b)$$

$$\left(\frac{k_{m0}}{k_{c,0}} \right)^t = \left(\frac{k_{m0}}{k_{c,0}} \right)^e \quad (45c)$$

Actually equation (45c) is automatically satisfied as long as equation (45a) is satisfied in conjunction with a relation previously discussed, namely,

$$\left(\frac{k_{c,0}}{k_0}\right)^t = \left(\frac{k_{c,0}}{k_0}\right)^e$$

Next consider the groups which would ensure similarity of the solid to solid radiation, the groups in equation (42) which contain the total hemispherical emissivity of the metal ϵ_m . The absorption factor $B_{m,j}$ depends on angle factors and the total hemispherical emissivities of all the solid surfaces which interact radiantly. Because of geometric similarity, corresponding angle factors in the test rig and in the engine are equal. If the same solid materials are used in both the test rig and the engine, approximate equality of corresponding emissivities is obtained unless the emissivities are very temperature dependent. In that case, the lower solid surface temperatures of the test rig as compared with the engine make equality of the emissivities difficult to obtain. However, these problems pale in comparison with the difficulties raised by the presence of T_0^4 in each of the radiation terms. For instance, strict similarity requires that

$$\left(\frac{\epsilon_m \sigma T_0^4}{k_0}\right)^t = \left(\frac{\epsilon_m \sigma T_0^4}{k_0}\right)^e \quad (45d)$$

Cancelling out the Stefan-Boltzmann constant σ and rearranging give

$$\frac{\epsilon_m^t}{\epsilon_m^e} = \frac{k_0^t}{k_0^e} \frac{(T_0^4)^e}{(T_0^4)^t} \quad (45e)$$

Despite the moderating influence of the thermal conductivity ratio, the temperature ratio to the fourth power dominates the right side of equation (45e) whenever the hot gas test rig temperature is markedly lower than the hot gas engine temperature. Obviously, equation (45e) can then easily require values of ϵ_m^t greater than 1 in order that equation (45d) be satisfied, but such values are thermodynamically forbidden. The difficulties involved in satisfying the radiation requirements for similarity are pointed out in reference 4.

Dropping all the radiation groups, as well as the other groups previously discussed, simplifies equation (42) and yields

$$\begin{aligned}
(U, V, W, \hat{P}, \theta, \hat{\rho}, \theta_m, U_c, V_c, W_c, \hat{P}_c, \theta_c, \hat{\rho}_c, K) = \\
= P_i \left(X, Y, Z, Re, Pr, M_\infty, \frac{w_{ci}}{U_\infty}, \frac{T_{ci}}{T_0}, \frac{P_{ci}}{P_\infty}, TI_\infty \right)
\end{aligned} \quad (46)$$

Thus, when air or gases like air are used for the test fluids and the same metal as in the engine is used in the test rig, approximate similarity between the test rig and the engine is enforced by equality of the nondimensional groups on the right side of equation (46) for the test rig and the engine.

Illustration of Scaling Procedure for Hot Gas Side Surface Coefficient of Heat Transfer

To understand how the method of differential similarity is used to predict engine performance based on available experimental results from the test rig, consider the problem of finding the engine gas side surface coefficient h^e when the measured values from the test h^t are available. One has, from the definition of h ,

$$h = - \frac{k \left(\frac{\partial T}{\partial n} \right)_{n=0}}{T_m - T_s} \quad (47)$$

where T_m is the local metal temperature, and T_s is a static temperature outside the boundary layer, or a local bulk mean temperature if the flow is not of the boundary-layer type, or an aerodynamic recovery temperature. This last choice is the one ordinarily made since it allows the high-speed h to be practically the same as the low-speed h . The precise choice of T_s is relatively unimportant to the discussion that follows as long as one is consistent when using the result. Utilizing equation (47) along with the definitions of N_o and θ causes (47) to become

$$h = - \frac{\frac{k_0}{L} \left(\theta^g \frac{\partial \theta}{\partial N_o} \right)_{N_o=0}}{\theta_m - \theta_s} \quad (48)$$

or after rearrangement

$$\frac{hL}{k_0} = - \frac{\left(\theta^g \frac{\partial \theta}{\partial N_o} \right)_{N_o=0}}{\theta_m - \theta_s} \quad (49)$$

If the groups on the right side of equation (46) are equal in the test rig and the engine, it then follows from equation (46) that θ_m , θ_s , and $(\partial\theta/\partial N_o)_{N_o=0}$ are exactly the same functions of the nondimensional space coordinates X , Y , and Z in both the test rig and the engine. Therefore, hL/k_0 has the same value at corresponding points for the test rig and the engine, and the following form is obtained for scaling purposes:

$$\frac{h^e_L}{k_0^e} = \frac{h^t_L}{k_0^t} \quad (50)$$

Equation (50) is used to predict h^e once h^t is measured. A similar procedure can be employed to scale coolant side conditions such as the surface coefficient and the wall shearing stress. Because of many analytical and experimental results (see refs. 6 and 7), it is well known that the local Nusselt number depends upon the molecular Prandtl number to about the one-third power, at least in the moderate Prandtl number range. This information can be used to write down the form equation (50) takes if strict Prandtl number similarity is not achieved:

$$\frac{h^e_L}{k_0^e} = \frac{h^t_L}{k_0^t} \left(\frac{Pr^e}{Pr^t} \right)^{1/3} \quad (51)$$

Equation (51) is essentially equivalent to equation (11) of reference 4, which evolves from physical insight arguments.

Reduction of Groups to More Useful Forms and Comparison

with Groups from References

Some of the groups on the right side of equation (46) are not in the form which is most easily controlled by the experimenter when he sets the test conditions that presumably effect similarity between the test rig and the engine. The tasks of reduction of groups to more useful forms, comparison with groups used by other investigators, and verification of the groups arrived at by other investigators are addressed next.

From equation (46) one of the requirements for similarity is that

$$Re^e = Re^t$$

or

$$\frac{\rho_{\infty}^e u_{\infty}^e L^e}{\mu_0^e} = \frac{\rho_{\infty}^t u_{\infty}^t L^t}{\mu_0^t} \quad (52)$$

Another is that

$$M_{\infty}^e = M_{\infty}^t$$

These lead to

$$\frac{u_{\infty}^e}{u_{\infty}^t} = \frac{c_{\infty}^e}{c_{\infty}^t} \quad (53)$$

The perfect gas equation of state and equation (53) inserted into (52) yield

$$\frac{R^t}{R^e} \frac{P_{\infty}^e}{P_{\infty}^t} \frac{c_{\infty}^e}{c_{\infty}^t} \frac{L^e}{L^t} \frac{T_{\infty}^t}{T_{\infty}^e} \frac{\mu_0^t}{\mu_0^e} = 1 \quad (54)$$

Using the relation for c_{∞} and T_0/T_{∞} developed in appendix C, the fact that

$$\left(\frac{c_{p,\infty}}{R} \right)^t = \left(\frac{c_{p,\infty}}{R} \right)^e \quad (55)$$

from equation (42), and the result that

$$\left(\frac{P_0}{P_{\infty}} \right)^e = \left(\frac{P_0}{P_{\infty}} \right)^t \quad (56)$$

(which can be shown) enables one to rewrite equation (54) as

$$\frac{P_0^t \mu_0^e}{P_0^e \mu_0^t} \sqrt{\frac{T_0^e}{T_0^t}} \sqrt{\frac{R^e L^t}{R^t L^e}} = 1 \quad (57)$$

However, since a power law dependence of viscosity upon temperature was postulated, it can be easily shown that

$$\frac{\mu_0^e}{\mu_0^t} = \frac{\mu_\infty^e}{\mu_\infty^t} \quad (58)$$

Combining equations (57) and (58) yields

$$\frac{P_0^t \mu_\infty^e}{P_0^e \mu_\infty^t} \sqrt{\frac{R^e T_0^e L^t}{R^t T_0^t L^e}} = 1 \quad (59)$$

Equation (59) and its equivalent (57) are consequences of the equalities (52), (53), and (55) predicted by the method of differential similarity. Equation (57), in particular, is useful for finding the required P_0^t for similarity. Ordinarily one would know P_0^e , T_0^e , R^e , R^t , and L^t/L^e ; would choose a T_0^t less than T_0^e ; would determine μ_0^t and μ_0^e from property tables; and would then solve equation (57) for P_0^t , a quantity easily controlled and set by the investigator in the test rig.

Comparing equation (59) with equation (5) of reference 4, one sees that they are identical once L^t/L^e is set equal to unity (because the ref. 4 equation is based on full-scale hardware) and once Γ^t/Γ^e in reference 4 is set equal to unity. The latter ratio is a function of the specific heat ratios in test rigs and engines, and the similarity requirement of equation (55) forces the specific heat ratio to be unity. Equation (5) of reference 4 is derived by the approach previously referred to as a heuristic, physical insight combined with experience and knowledge type of approach. The differential similarity analysis which led to equation (59) serves as a more rigorous basis for and substantiation of the physical approach.

Using expressions for the various mass flow rates, the perfect gas equation of state, the similarity requirements of equation (46) or (42), particularly the requirements

$$\frac{w_{ci}^t}{u_\infty^t} = \frac{w_{ci}^e}{u_\infty^e} \quad (60)$$

$$\frac{P_{ci}^t}{P_{\infty}^t} = \frac{P_{ci}^e}{P_{\infty}^e} \quad (61)$$

and

$$\frac{T_{ci}^t}{T_0^t} = \frac{T_{ci}^e}{T_0^e} \quad (62)$$

one can show that there results

$$\frac{\omega_c^t}{\omega^t} = \frac{\omega_c^e}{\omega^e} \quad (63)$$

Thus, the ratio of coolant mass flow rate to hot gas mass flow rate in the test rig must equal the mass flow rate ratio in the engine. This consequence of the differential similarity analysis is often used as a starting point in some of the more physical approaches to similarity as, for instance, in reference 1. Equation (63) also agrees exactly with its equivalent in reference 4, which is derived there as a byproduct of another physical requirement.

One can also show from the similarity requirements, equation (46) or (42), that at corresponding points in the flow (such as a film cooling slot, for instance) the momentum thickness Reynolds numbers, momentum flux ratios, and mass flux ratios are the same in the test rig as in the engine. That is,

$$Re_{\delta_i}^t = Re_{\delta_i}^e \quad (64)$$

$$\left(\frac{\rho_c V_c^2}{\rho V^2} \right)^e = \left(\frac{\rho_c V_c^2}{\rho V^2} \right)^t \quad (65)$$

$$\left(\frac{\rho_c |\vec{V}_c|}{\rho |\vec{V}|} \right)^e = \left(\frac{\rho_c |\vec{V}_c|}{\rho |\vec{V}|} \right)^t \quad (66)$$

where $|\vec{V}|$ is the magnitude of the nondimensional velocity vector \vec{V} , and terms like V^2 are to be interpreted as the vector dot product, $V^2 = \vec{V} \cdot \vec{V}$, not as the square of the nondimensional Y component of this vector. Requirements (64), (65), and (66) along with

geometric similarity assure the same adiabatic film effectiveness in the test rig and in the engine. By way of contrast, reference 4 asserts it is self-evident that equalities (64), (65), and (66) are physically reasonable requirements to force similarity. Finally, it can be shown that the similarity requirements (eq. (46) or (42)) lead to equation (9) of reference 4 and to the result that φ (a commonly used dimensionless wall temperature) is the same in both the test rig and the engine:

$$\varphi^e = \varphi^t \quad (67)$$

Hence, the heuristic, physical insight approach to similarity constraints as advanced in reference 4 is totally verified by the present work, which represents a more rigorous, more mathematical approach to the similarity problem. The present work predicts the need to maintain the same turbulence intensity in both the test rig and the engine, as does reference 4 also. In addition, the method of differential similarity predicts numerous other groups, on the right side of equation (42), that theoretically should be held constant between the test rig and the engine. These other groups, some of which have not appeared in the other references, most likely are of second order effect in most instances for the reasons noted previously. They could, however, assume a greater importance if any drastic changes were made in the types of fluids and metals used in the test rig relative to the types used in the engine.

Equations (57) and (62) are two of the most useful results of this report for the determination of what pressure and temperature levels to set in the test rig to achieve similarity with the engine. However, since these equations are equivalent to the relations in reference 4, it is recommended that the reader follow the procedure given in reference 4 to set the test conditions. Representative numerical calculations employing equations (57) and (62) have been made by the author, and agreement is good when compared with the similarity states given in table II of reference 4. The very slight differences can be traced to the slightly different viscosity-temperature relations used and the fact that reference 4 makes a correction for the small difference in specific heat ratios between test rig and engine conditions whereas the method presented in this report does not. However, the correction for different specific heat ratios could be incorporated easily, since it did originally appear in the derivations, but was cancelled out by the similarity requirement (55).

SUMMARY OF RESULTS

The method of differential similarity was used to rigorously derive nondimensional groups that are sufficient to ensure that the nondimensional fields of temperature, velocity, pressure, and density are the same in both a test rig and an engine for the hot

gas, coolant, and metal components. The following results were obtained:

1. Arguments were given based on available experimental evidence and on the usual choice of types of fluids and metal used; these arguments reduce the large number of nondimensional parameters sufficient for similarity to a much smaller necessary number of groups for approximate similarity in many cases.

2. It was shown that approximate similarity, both aerodynamic and thermal, can be achieved in a similar geometry if the inlet Mach number, Reynolds number, ratio of coolant temperature to hot gas stagnation temperature, ratio of coolant to hot gas mass flow rate, Prandtl number, and free-stream turbulence intensity in the test rig are set equal to their counterparts in the engine.

3. The derivation and the results presented serve as a proof of the validity of the similarity groups proposed by earlier investigators using heuristic, physical insight arguments.

4. The method when applied to some simple turbulence models predicts additional groups needed for similarity in steady turbulent flow, although only one of them, the turbulence intensity, is thought to be important to the usual type of experiment.

Lewis Research Center,

National Aeronautics and Space Administration,

Cleveland, Ohio, November 2, 1976,

505-04.

APPENDIX A

SYMBOLS

$B_{m,j}$	absorption factor
b	exponent
C_D	constant related to dissipation of turbulent kinetic energy
c	local speed of sound
c_p	specific heat at constant pressure
d	exponent
Ec	Eckert number
Eu	Euler number
F_j	function
f_1, f_2, f_3	functions
G_1	function
g	exponent
h	surface coefficient of heat transfer
i	static enthalpy per unit mass
i_0	stagnation enthalpy per unit mass
j	index
K	nondimensional time-averaged turbulent kinetic energy
k	thermal conductivity
L	airfoil chord
L_{mix}	mixing length
l	exponent
M	Mach number
m_0	nondimensional space coordinate measured perpendicularly outward from metal surface into coolant
n	space coordinate measured perpendicularly outward from metal surface into hot gas
N_0	nondimensional n

P	local pressure
P_i	function
\hat{P}	nondimensional pressure
Pr	Prandtl number
p	number of radiation surfaces on hot gas side
p_c	number of radiation surfaces on coolant side
R	particular gas constant
Re	Reynolds number
S	entropy per unit mass
T	static temperature (absolute)
T_0	stagnation temperature (absolute) of hot gas at inlet
TI_∞	turbulence intensity at inlet
U	nondimensional x-component of velocity
u	x-component of velocity
V	nondimensional y-component of velocity
v	y-component of velocity
W	nondimensional z-component of velocity
w	z-component of velocity
X	nondimensional x-coordinate
x	space coordinate
Y	nondimensional y-coordinate
y	space coordinate
Z	nondimensional z-coordinate
z	space coordinate
Γ	function of γ
γ	specific heat ratio
Δ	nondimensional velocity boundary-layer thickness
δ	local thickness of velocity boundary layer
δ_1	local momentum thickness
ϵ	total hemispherical emissivity

θ	temperature ratio, T/T_0
μ	dynamic viscosity
ξ	dummy variable for T
ρ	mass density
$\hat{\rho}$	nondimensional density
σ	Stefan-Boltzmann constant
σ_k	effective Prandtl number for diffusion of turbulent kinetic energy
σ_t	turbulent Prandtl number
τ	shearing stress
Φ	dissipation function
ω	mass flow rate

Subscripts:

c	coolant
ci	coolant inlet
i	index
m	metal
m0	metal condition at hot gas inlet stagnation temperature
ref	reference state
s	undisturbed conditions far from surface
t	turbulent
x	x-direction
0	stagnation conditions at hot gas inlet
∞	static condition of hot gas at inlet

Superscripts:

e	engine (prototype)
t	test or test rig (model)

APPENDIX B

ILLUSTRATION OF DIFFERENTIAL SIMILARITY

APPLIED TO MOMENTUM EQUATION

Equation (2) is the x -direction Navier-Stokes equation for the hot gas, and equation (6) is the viscosity-temperature relation for the hot gas. When these equations are combined, and only one of the viscous stresses is retained explicitly (because the others do not add any new nondimensional groups), the result is

$$\rho \left(u \frac{\partial u}{\partial x} + v \frac{\partial u}{\partial y} + w \frac{\partial u}{\partial z} \right) = - \frac{\partial P}{\partial x} + \frac{\partial}{\partial y} \left[\mu_0 \left(\frac{T}{T_0} \right)^d \frac{\partial u}{\partial y} + \dots \right] + \dots \quad (B1)$$

Equation (B1) is transformed to nondimensional dependent variables by introducing the following definitions:

$$\begin{aligned} \theta &= \frac{T}{T_0} & W &= \frac{w}{u_\infty} \\ U &= \frac{u}{u_\infty} & \hat{P} &= \frac{P}{P_\infty} \\ V &= \frac{v}{u_\infty} & \hat{\rho} &= \frac{\rho}{\rho_\infty} \end{aligned}$$

Inserting these into equation (B1) gives

$$\rho_\infty u_\infty^2 \hat{\rho} \left(U \frac{\partial U}{\partial x} + V \frac{\partial U}{\partial y} + W \frac{\partial U}{\partial z} \right) = -P_\infty \frac{\partial \hat{P}}{\partial x} + \mu_0 u_\infty \frac{\partial}{\partial y} \left(\theta^d \frac{\partial U}{\partial y} + \dots \right) + \dots \quad (B2)$$

Next the independent variables are formally transformed from x , y , and z to X , Y , and Z , where

$$X = \frac{x}{L}$$

$$Y = \frac{y}{L}$$

$$Z = \frac{z}{L}$$

Thus, viewing $U = U(X, Y, Z)$, one has

$$dU = \frac{\partial U}{\partial X} dX + \frac{\partial U}{\partial Y} dY + \frac{\partial U}{\partial Z} dZ \quad (B3)$$

Hence, from equation (B3) it follows that

$$\frac{\partial U}{\partial x} = \frac{\partial U}{\partial X} \frac{\partial X}{\partial x} = \frac{1}{L} \frac{\partial U}{\partial X} \quad (B4)$$

and similarly for the other derivatives. Then equation (B2) becomes

$$\frac{\rho_\infty u_\infty^2}{L} \hat{\rho} \left(U \frac{\partial U}{\partial X} + V \frac{\partial U}{\partial Y} + W \frac{\partial U}{\partial Z} \right) = -\frac{P_\infty}{L} \frac{\partial \hat{P}}{\partial X} + \frac{\mu_0 u_\infty}{L^2} \frac{\partial}{\partial Y} \left(\theta^d \frac{\partial U}{\partial Y} + \dots \right) + \dots \quad (B5)$$

Finally, (B5) is made nondimensional by dividing every term by $\rho_\infty u_\infty^2/L$ to obtain

$$\hat{\rho} \left(U \frac{\partial U}{\partial X} + V \frac{\partial U}{\partial Y} + W \frac{\partial U}{\partial Z} \right) = -Eu \frac{\partial \hat{P}}{\partial X} + \frac{1}{Re} \frac{\partial}{\partial Y} \left(\theta^d \frac{\partial U}{\partial Y} + \dots \right) + \dots \quad (B6)$$

where

$$Eu = \frac{P_\infty}{\rho_\infty u_\infty^2}$$

$$Re = \frac{\rho_\infty u_\infty L}{\mu_0}$$

APPENDIX C

RELATIONS INVOLVING MACH NUMBER M_∞

The hot gas inlet Mach number and the stagnation enthalpy at the inlet are by definition

$$M_\infty = \frac{u_\infty}{c_\infty} \quad (C1)$$

$$i_0 = i_\infty + \frac{u_\infty^2}{2} \quad (C2)$$

But for the case where the enthalpy per unit mass depends only on temperature

$$i_0 - i_\infty = \int_{T_\infty}^{T_0} c_p(\xi) d\xi \quad (C3)$$

The power law representation of the relation between specific heat and temperature is, in terms of the dummy variable ξ ,

$$c_p(\xi) = c_{p,\infty} \left(\frac{\xi}{T_\infty} \right)^l \quad (C4)$$

Performing the indicated operations and combining equations (C2) to (C4) give

$$u_\infty^2 = \frac{2T_\infty c_{p,\infty}}{l+1} \left[\left(\frac{T_0}{T_\infty} \right)^{l+1} - 1 \right] \quad (C5)$$

The local speed of sound c is

$$c = \sqrt{\left(\frac{\partial P}{\partial \rho} \right)_s} \quad (C6)$$

Using the combined first and second laws of thermodynamics results in

$$T dS = di - \frac{1}{\rho} dP \quad (C7)$$

But

$$di = c_{p, \infty} \left(\frac{T}{T_{\infty}} \right)^l dT \quad (C8)$$

and differentiating the perfect gas equation of state gives

$$dT = \frac{dP}{R\rho} - \frac{P}{\rho^2 R} d\rho \quad (C9)$$

Inserting equations (C8) and (C9) into (C7) and setting $dS = 0$, one can solve for the right side of equation (C6) and find

$$c_{\infty}^2 = \frac{c_{p, \infty} T_{\infty}}{\frac{c_{p, \infty}}{R} - 1} \quad (C10)$$

Combining equations (C1), (C6), and (C10) yields

$$M_{\infty}^2 = \frac{2 \left(\frac{c_{p, \infty}}{R} - 1 \right) \left[\left(\frac{T_0}{T_{\infty}} \right)^{l+1} - 1 \right]}{l + 1} \quad (C11)$$

Solving equation (C11) for T_0/T_{∞} gives, in implicit functional form,

$$\frac{T_0}{T_{\infty}} = f_1 \left(M_{\infty}, \frac{c_{p, \infty}}{R}, l \right) \quad (C12)$$

The Euler number is defined by

$$Eu = \frac{P_{\infty}}{\rho_{\infty} u_{\infty}^2} \quad (C13)$$

Using the perfect gas equation of state and equation (C5) in (C13) leads to

$$Eu = \frac{l + 1}{2 \frac{c_{p, \infty}}{R} \left[\left(\frac{T_0}{T_\infty} \right)^l - 1 \right]} \quad (C14)$$

Taking cognizance of equation (C12), one can write equation (C14), in implicit form, as

$$Eu = f_2 \left(M_\infty, \frac{c_{p, \infty}}{R}, l \right) \quad (C15)$$

The Eckert number is defined by

$$Ec = \frac{u_\infty^2}{c_{p, \infty} T_0} \quad (C16)$$

Combining equations (C5) and (C16) results in

$$Ec = \frac{2}{l + 1} \frac{T_\infty}{T_0} \left[\left(\frac{T_0}{T_\infty} \right)^{l+1} - 1 \right] \quad (C17)$$

Hence, equation (C17), in implicit form, can be written as

$$Ec = f_3 \left(M_\infty, \frac{c_{p, \infty}}{R}, l \right) \quad (C18)$$

REFERENCES

1. Gladden, Herbert J.; and Livingood, John N. B.: Procedure for Scaling of Experimental Turbine Vane Airfoil Temperatures From Low to High Gas Temperatures. NASA TN D-6510, 1971.
2. Schlichting, Hermann (J. Kestin, trans.): Boundary Layer Theory. 4th ed., McGraw-Hill Book Co., Inc., 1962.
3. Colladay, Raymond S.: Turbine Cooling. Ch. 11 in Turbine Design and Application, vol. 3, Arthur J. Glassman, ed., NASA SP-290, 1975, pp. 59-101.
4. Colladay, Raymond S.; and Stepka, Francis S.: Similarity Constraints in Testing of Cooled Engine Parts. NASA TN D-7707, 1974.
5. Eckert, Ernst R. G.; and Drake, Robert M., Jr.: Heat and Mass Transfer. 2nd ed., McGraw-Hill Book Co., Inc., 1959.
6. Sucec, James: Heat Transfer. Simon and Schuster, Inc., 1975.
7. Kays, William M.: Convective Heat and Mass Transfer. McGraw-Hill Book Co., Inc., 1966.
8. Launder, B. E.; and Spalding, D. B.: Lectures in Mathematical Models of Turbulence. Academic Press, 1972.

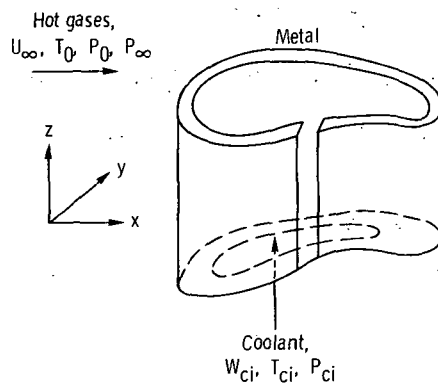


Figure 1. - Schematic drawing of air-cooled vane.



POSTMASTER : If Undeliverable (Section 158
Postal Manual) Do Not Return

"The aeronautical and space activities of the United States shall be conducted so as to contribute . . . to the expansion of human knowledge of phenomena in the atmosphere and space. The Administration shall provide for the widest practicable and appropriate dissemination of information concerning its activities and the results thereof."

—NATIONAL AERONAUTICS AND SPACE ACT OF 1958

NASA SCIENTIFIC AND TECHNICAL PUBLICATIONS

TECHNICAL REPORTS: Scientific and technical information considered important, complete, and a lasting contribution to existing knowledge.

TECHNICAL NOTES: Information less broad in scope but nevertheless of importance as a contribution to existing knowledge.

TECHNICAL MEMORANDUMS: Information receiving limited distribution because of preliminary data, security classification, or other reasons. Also includes conference proceedings with either limited or unlimited distribution.

CONTRACTOR REPORTS: Scientific and technical information generated under a NASA contract or grant and considered an important contribution to existing knowledge.

TECHNICAL TRANSLATIONS: Information published in a foreign language considered to merit NASA distribution in English.

SPECIAL PUBLICATIONS: Information derived from or of value to NASA activities. Publications include final reports of major projects, monographs, data compilations, handbooks, sourcebooks, and special bibliographies.

TECHNOLOGY UTILIZATION PUBLICATIONS: Information on technology used by NASA that may be of particular interest in commercial and other non-aerospace applications. Publications include Tech Briefs, Technology Utilization Reports and Technology Surveys.

Details on the availability of these publications may be obtained from:

SCIENTIFIC AND TECHNICAL INFORMATION OFFICE

NATIONAL AERONAUTICS AND SPACE ADMINISTRATION

Washington, D.C. 20546